Preparation and transport properties of polycrystalline Bi and Bi–SiO2 nanocomposites

F. Brochin, Bertrand Lenoir, X. Devaux, R. Martin-Lopez, H. Scherrer

Preparation and transport properties of polycrystalline Bi and $Bi–SiO_2$ nanocomposites

Cite as: Journal of Applied Physics **88**, 3269 (2000); https://doi.org/10.1063/1.1289079
Submitted: 30 March 2000 • Accepted: 20 June 2000 • Published Online: 30 August 2000

F. Brochin, B. Lenoir, X. Devaux, et al.

Preparation and transport properties of polycrystalline Bi and Bi–SiO_2 nanocomposites

F. Brochin, B. Lenoir,[a] X. Devaux, R. Martin-Lopez, and H. Scherrer
Laboratoire de Physique des Matériaux, UMR CNRS 7556, Ecole des Mines, 54 042 Nancy Cedex, France

(Received 30 March 2000; accepted for publication 20 June 2000)

Bismuth–silica nanocomposites and polycrystalline bismuth were prepared via powder metallurgy in order to study the influence of silica inclusions on the thermoelectric properties of bismuth. Bi–SiO_2 powders containing from 0.5 to 15 vol. % of silica and pure Bi powders were produced by an arc-plasma processing. Transmission electron microscopy investigations revealed the presence of a nanometric silica shell around the Bi grains. The powders were cold pressed and sintered close to the melting temperature of bismuth. The bulk microstructures are very different for the bismuth and the Bi–SiO_2 nanocomposites because silica, which is primarily dispersed at grain boundaries, inhibits the grain growth during sintering. The electrical resistivity was measured from 5 to 300 K, while the thermoelectric power and the thermal conductivity were measured from 65 to 300 K on both polycrystalline bismuth and Bi–SiO_2 samples containing 0.5, 4, and 15 vol. % of silica, respectively. The transport properties are mainly discussed with regard to the microstructures. In spite of a strong reduction of the thermal conductivity for the nanocomposites, the thermoelectric figure of merit is not improved compared to bismuth due to a dominating concurrent increase of the electrical resistivity resulting from a finite-size effect. © *2000 American Institute of Physics.* [S0021-8979(00)02419-1]

I. INTRODUCTION

The efficiency of a thermoelectric material at a specified temperature T depends on the product ZT,[1] where Z is the thermoelectric figure of merit of the material. This figure of merit is related to the transport properties by

$$Z = \frac{\alpha^2}{\rho\lambda}, \tag{1}$$

where α is the thermoelectric power (or Seebeck coefficient), ρ the electrical resistivity, and λ the thermal conductivity. The thermoelectric material is all the more performing if its figure of merit is high.

Bismuth-based semiconducting alloys are well known for their good thermoelectric properties. Bismuth telluride-based alloys are efficient at room temperature and commonly used for Peltier refrigeration, but their figure of merit dramatically decreases below 200 K and renewed interest has been shown in materials such as bismuth–antimony alloys[2–4] whose thermoelectric performance can be improved by applying a magnetic field.[5] However, the practical use of Bi-rich Bi–Sb single crystals in low temperature stages of solid state coolers is limited because single crystals cannot withstand any bending along their trigonal axis. Unfortunately, it is precisely in that direction that the figure of merit is the best. In order to improve the durability of the material, polycrystalline Bi–Sb alloys have been prepared via powder metallurgy in the last few decades. Several works were devoted to studying the influence of the microstructure on the thermoelectric properties.[6–8] It was concluded that the presence of grain boundaries reduced the thermal conductivity but it also gave rise to a sharp concurrent increase of the electrical resistivity. As a result, the figure of merit was lower for polycrystalline alloys than for single crystals.

Theoretical works[9,10] have recently predicted that the inclusion of particles of a few nanometers in a polycrystalline material could be an interesting way to obtain a significant improvement of the figure of merit. If the nanoinclusions are randomly dispersed throughout the materials, they could act as phonon scattering centers and the thermal conductivity should be considerably reduced. The electrical resistivity should not be greatly enhanced if the matrix grains are sufficiently large. These effects were successfully observed on Si–Ge alloys containing 4-to 10-nm particles.[11] Ideally, one would like to improve the figure of merit of Bi–Sb alloys in a similar manner, if possible. However, the electrical and thermal properties of these alloys strongly depend on the antimony content,[2–4] so that the effect of inclusions could be masked by other factors like chemical heterogeneity. We have, therefore, focused our attention on the pure component bismuth.

In order to enhance the figure of merit, the nanoinclusions must be insulating,[12] chemically stable in the temperature range of utilization of the material,[11] and inert with regard to the matrix.[13] To satisfy these selection criteria, refractor oxides are the best candidates. Therefore, we chose to disperse silica nanoinclusions in a polycrystalline bismuth matrix. Such structures, containing two phases, one of which is in the nanometer range, are called nanocomposites. These nanocomposites are usually prepared via powder metallurgy[14] which involves mixing two kinds of powders and sintering. The production of nanocomposite ultrafine powders by simultaneous evaporation, nucleation, and

[a]Electronic mail: lenoir@mines.u-nancy.fr

growth in the same place is also an attractive way to incorporate nanoinclusions in a material.[15–18]

In this work, we used an arc-plasma process to prepare pure polycrystalline bismuth and bismuth–silica nanocomposites. We first present the preparation of the materials while the second part is devoted to the study of their transport properties.

II. EXPERIMENTAL PROCEDURE

Bi and Bi–SiO_2 nanocomposite powders were prepared by arc-plasma processing. The technique used was already described in a previous article.[19] Bi pieces were evaporated alone or with silica targets under pure argon atmosphere in a dc arc flame. The powders were collected in a glove box under purified argon atmosphere (H_2O and $O_2<1$ ppm).

Chemical analyses of the powders were performed by inductive coupling plasma atomic emission spectroscopy. The morphology of the powders was observed using scanning electron microscopy (SEM). The microstructure observations of the powders and the phase identification were performed by conventional transmission electron microscopy (TEM) associated with x-ray energy dispersive spectrometry (XEDS) and electron energy loss spectrometry (EELS). The powders were introduced into an epoxy resin and thin slices (thinner than 100 nm) were prepared by ultramicrotomy. These slices were deposited on a 200-mesh copper grid and strengthened with a thin layer of carbon before observation.

Pellets, with 13-mm diameter and a thickness of 3 mm, were prepared by cold pressing the powders in a stainless steel die under vacuum at 600 MPa. This compacting stage was done with fresh powders, in the glove box where the powders are collected. The greens were then annealed for 24 h at 250 °C in vacuum or in an hydrogen stream. The bulk density was determined by the Archimedes method. SEM observations were carried out on fracture surfaces.

The microstructure of the sintered samples was also studied by TEM on samples prepared by successively mechanical and ion thinning.

Transport property measurements were performed on polycrystalline Bi and Bi–SiO_2 samples within the 65–300 K temperature range. Small parallelepipeds (typical dimensions were $2\times2\times10\,mm^3$) were cut with a wire saw from the sintered pellets. Electrical resistivity, thermoelectric power, and thermal conductivity were measured on the same sample. The experimental setup has been previously described in details elsewhere.[7] Both the thermal and electric gradients were applied perpendicular to the press direction. The thermal conductivity and the thermopower were measured by means of a four probe steady heater and sink method. The electrical resistivity was measured by the dc four probe method. Care was taken to eliminate any thermoelectric voltages. Additional electrical resistivity measurements were conducted down to helium temperature on some of the samples on an other experimental setup. For a sample measured in both setups, the measured temperature dependencies of the electrical resistivity perfectly coincide within the 65–300 K temperature range.

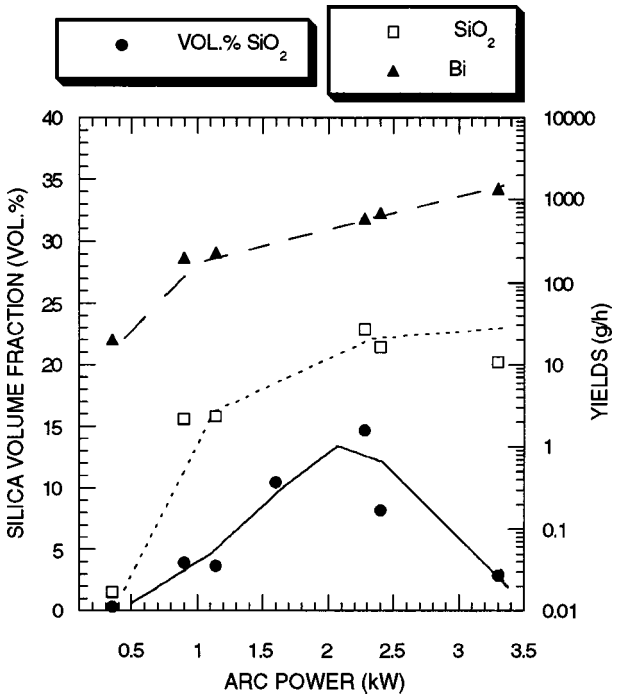

FIG. 1. Arc power dependence of the powder silica content and the evaporation yields of bismuth and silica.

III. PREPARATION OF THE MATERIALS

A. Powders

The heat transfer between the arc flame and the silica target is the determining factor that influences both the powder yield and the powder composition. The powder silica content can be controlled by the arc power. Figure 1 shows the dependence of the silica volume fraction on the arc power. Note that the volume fraction was determined from the silicon content given by the chemical analyses assuming the powders were only containing Bi and SiO_2. The behavior of the curve (Fig. 1) can be easily explained by considering the respective evaporation yields of bismuth and silica. In a previous work,[19] it was shown that the oxygen produced by the dissociation of silica in the arc ($T>10\,000$ K) catalyses the evaporation of bismuth. The amount of evaporated an dissociated silica increases with the arc power so that the evaporation yield of bismuth becomes much higher than that of silica when the arc power exceeds 2.5 kW. In addition, the silica volume fraction exhibits a maximum, which is about 15 vol. %.

SEM observations of the powders showed a bimodal grain size distribution, which was confirmed by Laser granulometry measurements. The first peak is centered on 1 μm and the second on 0.3 μm. The grains in the Bi powders are spherical. In the Bi–SiO_2 powders, the Bi grains were the only visible grains. The presence of silica does not affect their morphology. Their size depends on the evaporation yield as it is well known in a nucleation and growth process in vapor phase.

As silica grains in the powders could not be localized by SEM, we used TEM. On the micrographs (Fig. 2), two kinds of grains can be observed. The first are highly contrasted

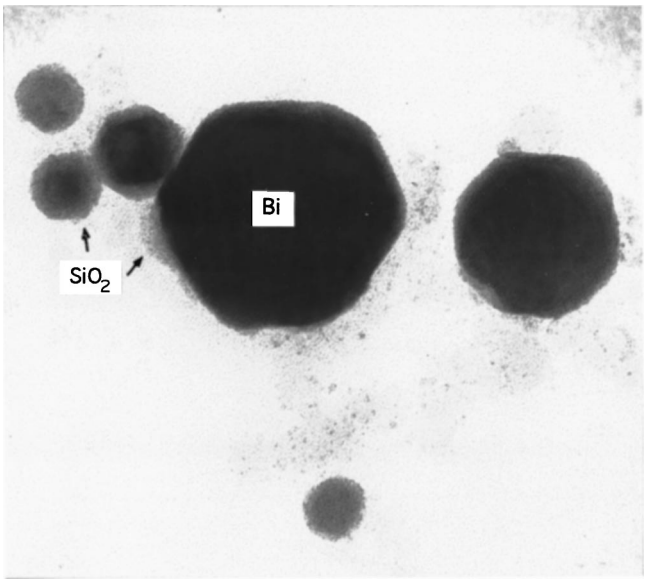

FIG. 2. TEM micrograph of a Bi 8 vol. % SiO_2 nanocomposite powder.

with a size going from 20 to 150 nm, and were identified as pure bismuth [Fig. 3(a)]. The second, whose size is about a few nanometers, are weakly contrasted. XEDS investigations [Fig. 3(b)] showed these small grains are constituted of silicon and oxygen (the additional $M\alpha$ peak is due to the surrounding bismuth). Figure 4 presents the Si L edge spectra for these small grains. The $L_{2,3}$ edge with an onset near 104 eV and a strongly peaked structure at 108, 115, and 130 eV and the L_1 edge with a peak at 160 eV are characteristic of pure silica.[20] These silica grains can form isolated aggregates but are primarily situated around the Bi grains. Careful observations show that each bismuth grain is systematically surrounded by a silica layer with a thickness of a few nanometers.

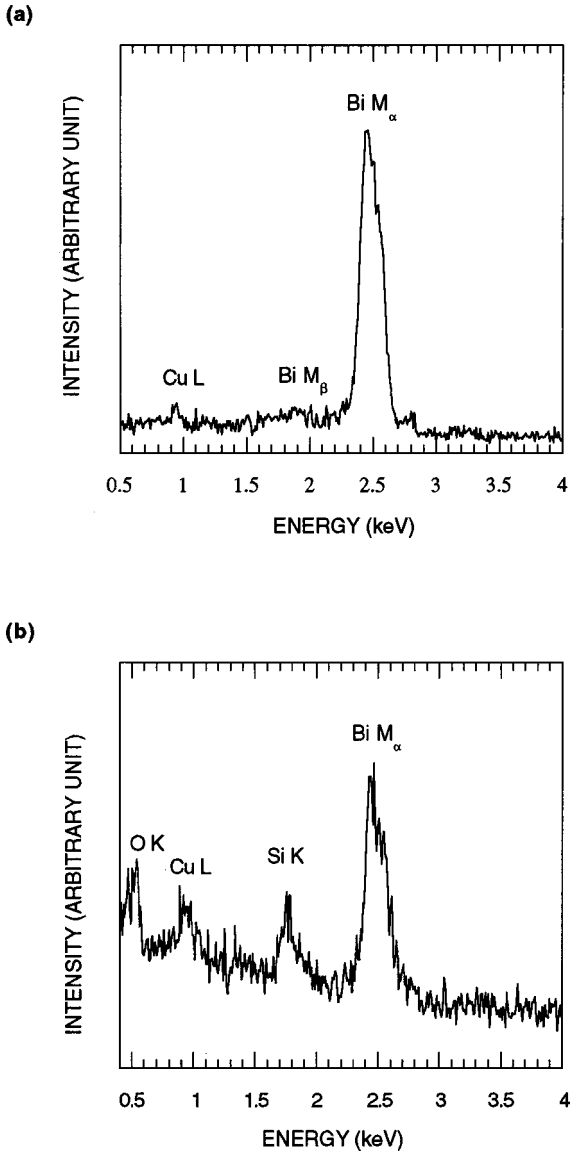

FIG. 3. XEDS spectra corresponding to (a) a bismuth grain and (b) silica grains. The Cu L peaks are due to the sample holder.

B. Bulk materials

The effect of sintering on the microstructure was studied on Bi compacts [Fig. 5(a)] for which the green relative density is higher than 0.95. For the samples sintered in vacuum, the relative density remains unchanged and the grain size never exceeds a few micrometers [Fig. 5(b)]. In order to avoid an enhancement of the electrical resistivity, polycrystalline materials with the largest grains possible must be prepared. To stimulate grain growth, the samples were sintered in a hydrogen atmosphere. After sintering, a grain size increase is obtained [Fig. 5(c)], but the relative density decreases to 0.80. This fact was explained by the presence of large pores [Fig. 5(d)] which are probably due to hydrogen trapped in the material during sintering that escapes later on. Porosity is harmful for thermoelectric properties because it leads to an enhancement of resistivity. As a result, it was decided to sinter the powders in vacuum.

Sintering the nanocomposite compacts at the same temperature as the bismuth leads to a grain size much smaller because the silica, which is situated around the bismuth grains, inhibits their growth. The sintering temperature was then increased up to 268 °C, i.e., 3° below the melting temperature of bismuth, but it had no significant influence on the grain size. In each case, the green relative density is higher than 0.95 before sintering and does not change during the process.

The microstructure of the sintered samples were studied using TEM. As shown by the micrographs in Fig. 6, the microstructures of polycrystalline bismuth and nanocomposites are very different. In polycrystalline bismuth, grains appear micrometric with a polygonal shape and no sign of porosity is observed. Whereas, in the nanocomposites, the grains remain spherical just as in the powders with a size that does not exceed a few hundred nanometers. Silica is primarily situated at the grain boundaries. The presence of inclusions containing silicon was also detected inside the grains. Nevertheless, the observation of these inclusions by TEM is difficult because of the high atomic number of bismuth and because of the large number of defects introduced in the grains during the preparation of the sample. The large voids between the grains are also probably created during this

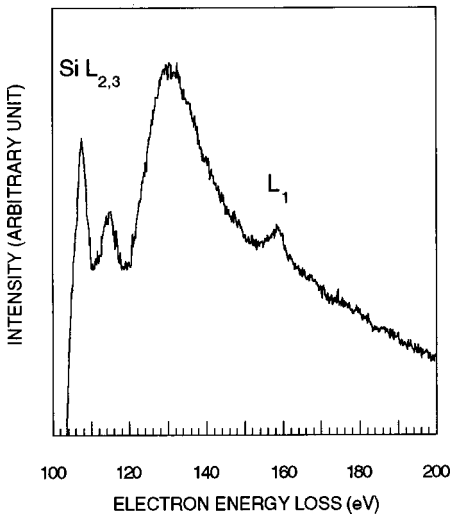

FIG. 4. EELS spectrum corresponding to silica grains.

preparation. One must, indeed, recall that since silica is not sintered the material is not well consolidated and it is likely to be damaged during thinning.

IV. TRANSPORT PROPERTIES

The study of the transport properties was performed for one Bi polycrystalline sample and three Bi–SiO_2 nanocomposite samples containing 0.5, 4, and 15 vol % of silica, respectively. The microstructure of the samples is described in Sec. III.

Because of the strong anisotropy of the Bi single crystals, we calculated average values of the transport coefficients, measured both along the trigonal axis and the basal planes, of a single crystal of Bi.[21,22] We compared this set of data for our polycrystalline Bi sample.

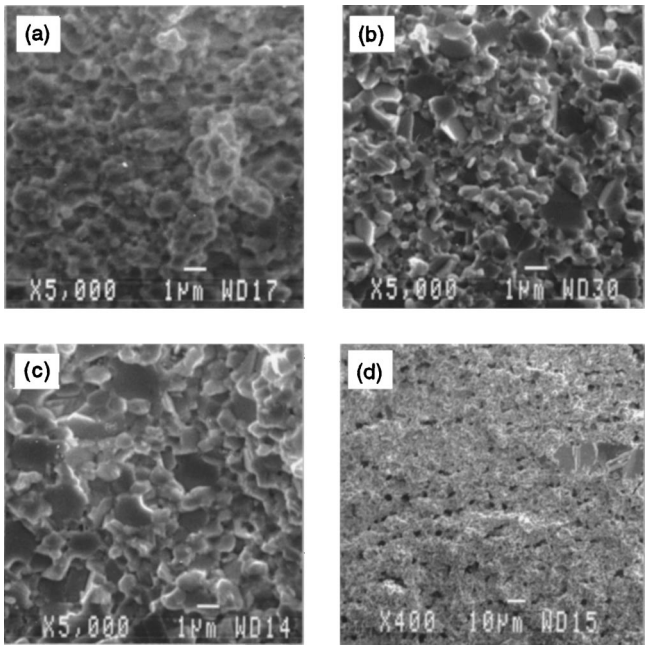

FIG. 5. SEM micrographs of bismuth pellets (a) as compacted (b) sintered under vacuum (c), and (d) sintered in an hydrogen atmosphere.

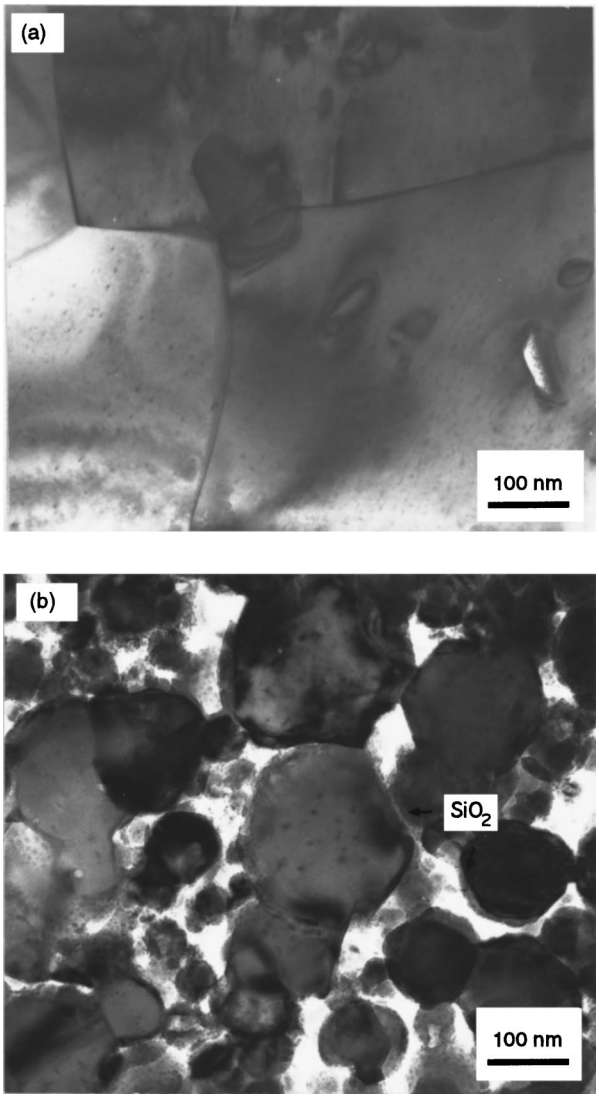

FIG. 6. TEM micrographs of (a) pure sintered Bi and (b) sintered Bi–SiO_2 nanocomposite.

The temperature dependencies of the electrical resistivity of the samples within the 4.2–300 K temperature range are shown in Fig. 7. The computed average values obtained with a Bi single crystal are also reported in this figure. [Note that below 50 K the two independent components measured parallel with (ρ_{33}) or perpendicular to (ρ_{11}) the trigonal axis are almost equal and at higher temperature the anisotropy (ρ_{33}/ρ_{11}) increases and is about 1.2 at 300 K.]

The values of the electrical resistivity of the Bi polycrystalline sample are quite constant and higher than the average value over the entire range of temperature. For the nanocomposites, the resistivity increases with decreasing temperature, i.e., the temperature coefficient of resistivity (TCR) is negative, and below 30 K the resistivity is practically temperature independent. It is noted that a negative TCR is also usually observed for Bi thin films and Bi nanowires[23,24] while it is positive for a Bi single crystal.

These different features can be qualitatively explained by referring to the opposite temperature dependencies of carrier concentration and mobility which contribute to the elec-

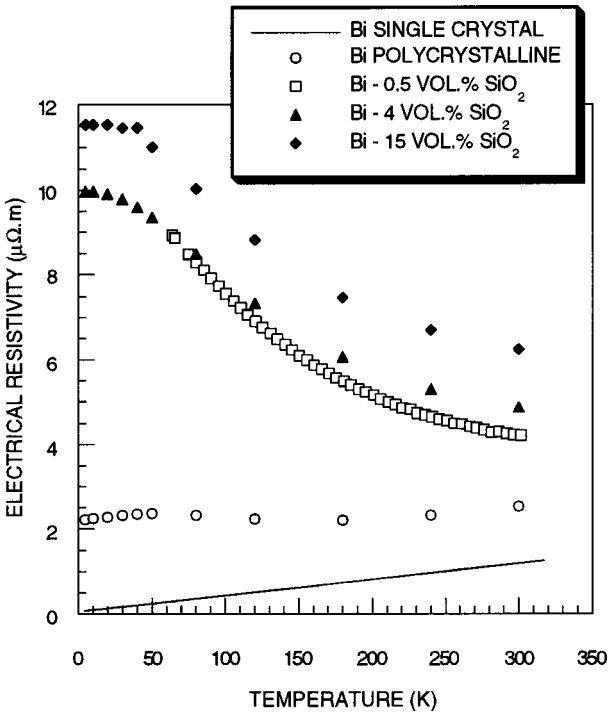

FIG. 7. Temperature dependence of the electrical resistivity of polycrystalline Bi and Bi–SiO_2 samples between 4.2 and 300 K. The line represents the computed average values for a Bi single crystal.

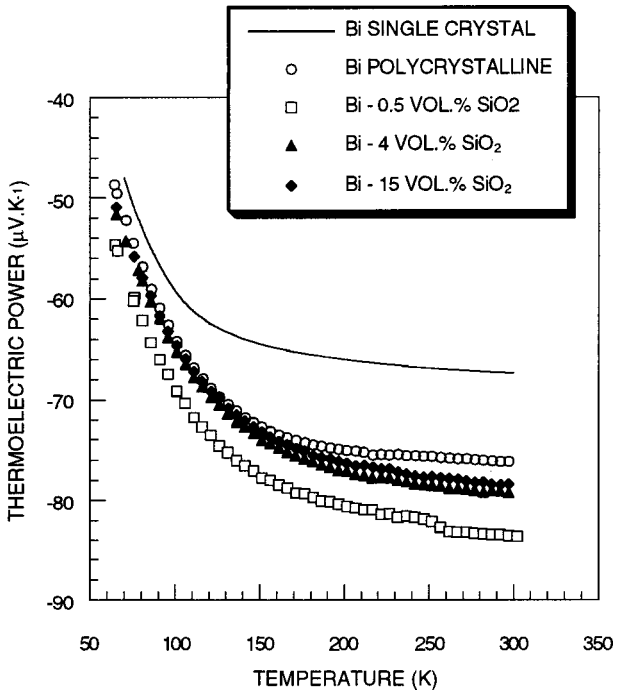

FIG. 8. Temperature dependence of the thermoelectric power of polycrystalline Bi and Bi–SiO_2 samples between 65 and 300 K. The line represents the computed average values for a Bi single crystal.

trical resistivity. In Bi single crystals, the carrier concentration increases as $T^{3/2}$ for $T>60\,\mathrm{K}$ whereas the carrier mobility follows a $T^{-5/2}$ variation.[25] Consequently, a metallic-like positive TCR is seen. In Bi thin films and in Bi nanowires, the mobility is suppressed by structural imperfection and finite size effects leading to a negative TCR due to the carrier concentration.[23,24] In the present case of polycrystalline Bi and Bi–SiO_2 nanocomposites, scattering at the grain boundaries is expected to be strong since the grain size, especially in the nanocomposites, is much less than the mean free path in the single crystals that could reach millimeter scale at low temperatures.[26,27] As a result, the carrier concentration dominates the TCR. Therefore, enhancement of the electrical resistivity for the nanocomposites can be ascribed to classical finite-size effects, as the mean free path is effectively limited by the crystallite boundaries. At low temperature, the carrier concentration and the mean free path, hence the electrical resistivity, become temperature independent.[27]

The increase of the silica volume fraction for the nanocomposites, which have similar grain size, leads only to a shift of the electrical resistivity. Klemens[10] has shown that the effect of insulating inclusions on the electrical resistivity is given by

$$\rho_2=\rho_1\left(1+\frac{4f}{3}\right), \tag{2}$$

where ρ_1 and ρ_2 are the electrical resistivity of single- and two-phase material, respectively, and f is the inclusions volume fraction. The relative variations for the Bi–SiO_2 observed in Fig. 5 are quite well described by Eq. (2).

In Fig. 8, thermoelectric power (TEP) values are plotted as a function of temperature for polycrystalline Bi and Bi–SiO_2 samples. The computed average values obtained with a Bi single crystal are also shown in this figure. (Note that in Bi single crystals, $\alpha_{33}\approx-100\,\mu\mathrm{V/K}^{-1}$ and $\alpha_{11}\approx-50\,\mu\mathrm{V/K}^{-1}$ for $80<T<300\,\mathrm{K}$ according to Gallo *et al.*[21])

For all the samples, the TEP is negative. As in single crystal, it is likely that this sign reflects the higher mobilities of electrons compared to those of holes. The variation of the TEP throughout the temperature range 65–300 K is quite the same as that for the average value of a single crystal. It increases (in absolute value) below 150 K and is quite constant at high temperatures. The values obtained for Bi polycrystalline are in good agreement with literature data.[28,29]

It should be noted that the absolute values of the TEP of the polycrystalline samples lie entirely above the average values of the Bi single crystal. For the nanocomposites, the presence of silica cannot, however, be responsible for such an increase of the TEP since, in the case of small volume fractions of insulating inclusions, it is well established that the TEP is not sensitive to that of inclusions.[30] Due to the large anisotropy of the thermopower the increased absolute value of the TEP could be linked to a preferential orientation of the grains. However, x-ray analysis do not show any texture. A possible explanation could be a charge-selective scattering mechanism which affects holes stronger than electrons. Scattering by potential barriers could contribute significantly.[31] The grain boundaries are known to be crystal regions containing many intrinsic defects (point or line defects, open bonds) or extrinsic defects (segregation, impurities). Consequently, potential barriers are formed at grain boundaries because the chemical potential is not the same in the grain boundary region as in the grains of the material.[32]

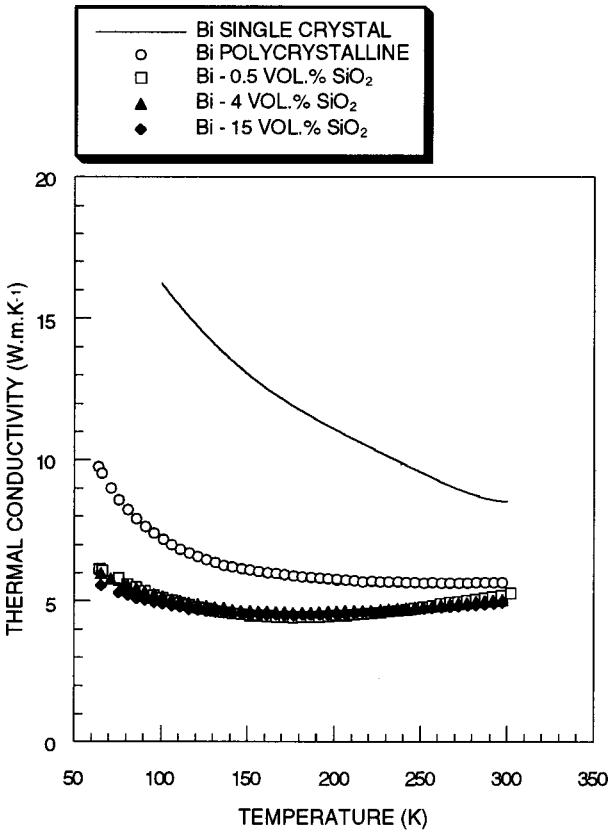

FIG. 9. Temperature dependence of the thermal conductivity of polycrystalline Bi and Bi–SiO_2 samples between 65 and 300 K. The line represents the computed average values for a Bi single crystal.

The enhancement of the TEP for the polycrystalline bismuth could be explained by the presence of such barriers. The effect is more pronounced for the nanocomposites since, first of all, the number of grain boundaries is more important, and secondly, the silica around the bismuth grains probably induces additional barriers.

Figure 9 presents the values measured for the thermal conductivity of polycrystalline Bi and Bi–SiO_2 samples, as well as the computed average values of the thermal conductivity of a single crystal of Bi are also reported (the anisotropy is near 2). The thermal conductivity of polycrystalline Bi is reduced in the whole temperature range compared to that of the single crystal.

In Bi, the thermal conductivity λ is principally the sum of two terms: an electronic contribution λ_E (including both unipolar and bipolar terms) and a contribution λ_L associated with the lattice vibrations (phonons)

$$\lambda = \lambda_E + \lambda_L . \tag{3}$$

Because of the low carrier concentration, heat in Bi is essentially carried by phonons.[33] These phonons have a very long mean free path, which can reach several hundred micrometers at 5 K,[34] and are consequently strongly scattered by extended defects. The strong reduction of thermal conductivity below 150 K for the polycrystal can thus be attributed to the presence of grain boundaries which limit the phonon mean free path. When the temperature increases, the phonon mean free path decreases and grain boundary scattering is less efficient, whereas the electronic contribution increases which explains the decrease of the slope.

The thermal conductivity of the Bi–SiO_2 nanocomposites is sharply reduced compared to that of polycrystalline bismuth. The addition of 0.5 vol. % of silica is sufficient to reduce the thermal conductivity by a factor 2. Increasing the volume fraction of silica from 0.5 to 15 vol. % seems to have no influence. The value for each nanocomposite is the same and is approximately 5 W/mK. It is quite surprising that the thermal conductivity of the Bi–SiO_2 does not depend on the volume fraction of silica. Theoretical calculations[35] predict that the addition of randomly dispersed nanoinclusions should lead to a progressive decrease of the thermal conductivity. This effect was experimentally confirmed on aluminum nitride containing silica inclusions.[36] In the case of our nanocomposites, microstructural investigations have clearly shown that the silica is primarily dispersed at the grain boundaries. Hence, we believe that the reduction of the thermal conductivity for the nanocomposites is not due to the phonon scattering expected. We may offer two possible explanations. The first is based on boundary scattering of phonons. Given the great difference of grain size between the polycrystalline Bi and the nanocomposites, boundary scattering of phonons will be more pronounced for the nanocomposites. This effect should be comparable for each nanocomposite since the grain size is almost the same. The second possible explanation is based upon mass-difference scattering. It was shown in a previous study[20] that silica was dissociated in the arc during the preparation of the powders. It can be envisaged that Si atoms substitute to Bi atoms. In this case, we would have to take into account a mass scattering which could affect the lattice vibrations. This effect is well established in the case of Bi–Sb solid solutions. Alloying bismuth with a small quantity of antimony (0.06 wt. %) leads to a noticeable decrease of the thermal conductivity.[37] Mass scattering is all the more intensive that the mass ratio of the two kinds of atom is high.[38] In the case of bismuth and antimony, this ratio equals 1.7 and it is more than 4 times higher for bismuth and silicon. The solubility of silicon in bismuth is very low (about 0.03 wt. %) but given the high mass ratio, the addition of even a small quantity of silicon to bismuth could explain the strong reduction of thermal conductivity for the Bi–SiO_2 nanocomposites. The high intensity of mass scattering could mask the other scattering mechanisms and thermal conductivity should then become insensitive to the volume fraction of silica.

The deduced figure of merit from previous results for polycrystalline bismuth and the three nanocomposites studied is reported Fig. 10. For polycrystalline bismuth, the figure of merit is much lower than the computed mean value of the single crystal below 150 K. At higher temperature, the measured value approaches that of the single crystal. In spite of the strong reduction of thermal conductivity and the increase (in absolute value) of the TEP, the figure of merit of the nanocomposites is lower than the polycrystalline bismuth's one due to a dominating concurrent increase of the electrical resistivity.

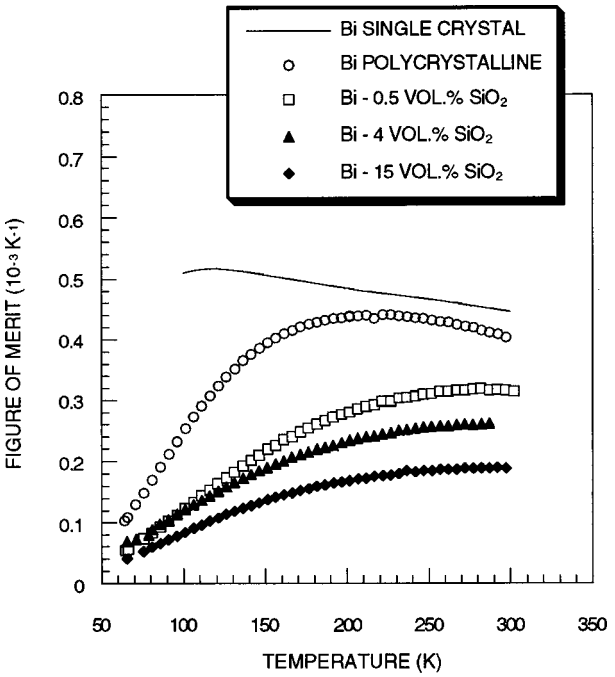

FIG. 10. Temperature dependence of the thermoelectric figure of merit of polycrystalline Bi and Bi–SiO_2 samples between 65 and 300 K. The line represents the computed average values for a Bi single crystal.

V. CONCLUSION

Bismuth–silica nanocomposites were prepared via powder metallurgy. Bi–SiO_2 ultrafine powders containing from 0.5 to 15 vol. % SiO_2 were obtained by an arc-plasma processing. TEM observations associated to EDS and EELS analyses revealed the presence of a silica shell around each Bi grain.

The powders were cold pressed and sintered under vacuum close to the melting temperature of bismuth. Bulk materials with relative density larger than 0.95 were obtained. The grain size is approximately a few micrometers for polycrystalline bismuth whereas it never exceeds a few hundred nanometers for Bi–SiO_2 samples since silica inhibits the grain growth during sintering.

The temperature dependence of the transport properties was studied for a pure Bi polycrystal and three Bi–SiO_2 composites containing 0.5, 4, and 15 vol. %, respectively, of silica. A strong increase of the electrical resistivity with a positive TCR was observed for the nanocomposites as a result of a finite-size effect. The thermoelectric power is increased (in absolute value) but the physical reason for this increase is not yet clearly understood. The thermal conductivity of the nanocomposites is significantly reduced compared to that of polycrystalline bismuth but is not sensitive to the silica volume fraction. The reduction is likely linked to grain boundary scattering but a possible mass scattering is not excluded. An enhanced figure of merit was not realized in these highly disordered systems due to a dominating concurrent increase of the electrical resistivity.

ACKNOWLEDGMENTS

The authors would like to thank Dr. J. Ghanbaja for EELS analyses and Dr. C. Bellouard for additional resistivity measurements performed at low temperatures. The authors are also very indebted to Dr. I. Vurgaftman and Dr. J. Meyer from the Naval Research Laboratory (Washington, DC) for fruitful discussions.

[1] H. G. Goldsmid, *Electronic Refrigeration* (Pion, London, 1986).
[2] G. E. Smith and R. Wolfe, J. Appl. Phys. **33**, 841 (1962).
[3] W. M. Yim and A. Amith, Solid-State Electron. **15**, 1141 (1972).
[4] B. Lenoir, M. Cassart, J. P. Michenaud, H. Scherrer, and S. Scherrer, J. Phys. Chem. Solids **57**, 89 (1996).
[5] R. Wolfe and G. E. Smith, Appl. Phys. Lett. **1**, 5 (1962).
[6] X. Devaux, F. Brochin, A. Dauscher, B. Lenoir, R. Martin-Lopez, H. Scherrer, and S. Scherrer, in Proceedings of the 16th International Conference on Thermoelectrics, Dresden, Germany, 1999, edited by A. Heinrich, p. 199.
[7] R. Martin-Lopez, A. Dauscher, H. Scherrer, J. Hejtmanek, H. Kenzari, and B. Lenoir, Appl. Phys. A: Mater. Sci. Process. **68**, 597 (1999).
[8] E. H. Volckmann, H. J. Goldsmid, and J. Sharp, in Proceedings of the Fifteenth International Conference on Thermoelectrics, Pasadena, CA, 1996, edited by T. Caillat, p. 22.
[9] G. A. Slack and M. A. Hussain, J. Appl. Phys. **70**, 2694 (1991).
[10] P. G. Klemens, Mater. Res. Soc. Symp. Proc. **234**, 87 (1991).
[11] N. Scoville, C. Bajgar, J. Rolfe, J. P. Fleurial, and J. Vandersande, Nanostruct. Mater. **5**, 207 (1995).
[12] J. P. Fleurial, in Proceedings of the 12th International Conference on Thermoelectrics, Yokohama, Japan, 1993, edited by K. Matsuura, p. 1.
[13] B. A. Cook, J. L. Harringa, and S. Loughlin, Mater. Sci. Eng., B **41**, 280 (1996).
[14] M. Sternitzke, J. Eur. Ceram. Soc. **17**, 1061 (1997).
[15] M. Uda and S. Ohno, Nippon Kagaku Kaishi **6**, 862 (1984).
[16] A. Inoue, B. G. Kim, K. Nosaki, T. Yamaguchi, and T. Masumoto, J. Appl. Phys. **71**, 4025 (1992).
[17] S. Ohno, K. Honma, H. Okuyama, and M. Ozawa, J. Jpn. Inst. Met. **53**, 936 (1989).
[18] X. Devaux, A. Thomy, and J. Ghanbaja, J. Mater. Sci. **32**, 4957 (1997).
[19] F. Brochin, X. Devaux, J. Ghanbaja, and H. Scherrer, Nanostruct. Mater. **11**, 1 (1999).
[20] P. E. Baston, Proceedings of Microscopy of Semiconducting Materials Conference, Oxford, UK, 1991, p. 55.
[21] C. F. Gallo, B. S. Chandrasekhar, and P. H. Sutter, J. Appl. Phys. **34**, 144 (1963).
[22] J. P. Issi, Aust. J. Phys. **32**, 585 (1979).
[23] R. Hoffman and D. R. Frankl, Phys. Rev. B **3**, 1825 (1971).
[24] K. Liu, C. L. Chien, P. C. Searson, and K. Yu-Zhang, Appl. Phys. Lett. **73**, 1436 (1998).
[25] J. P. Michenaud and J. P. Issi, J. Phys. C **5**, 3061 (1972).
[26] B. N. Aleksandrov, Sov. Phys. JETP **16**, 286 (1962).
[27] G. A. Ivanov and A. M. Papov, Sov. Phys. Solid State **5**, 1040 (1963).
[28] G. Cochrane and W. V. Youdelis, Metall. Trans. **3**, 2483 (1972).
[29] J. P. Issi, Ph. D. thesis, Louvain-La-Neuve, Belgium, 1965.
[30] D. J. Bergman and O. Levy, Mater. Res. Soc. Symp. Proc. **234**, 39 (1991).
[31] Yu. I. Ravich, *CRC Handbook of Thermoelectrics* (CRC, Boca Raton, FL, 1995), p. 67.
[32] C. H. Seager and T. G. Castner, J. Appl. Phys. **49**, 3879 (1978).
[33] S. Shalyt, J. Phys. (Moscow) **8**, 315 (1944).
[34] G. K. White and S. B. Woods, Philos. Mag. **3**, 342 (1958).
[35] C. B. Vining, Mater. Res. Soc. Symp. Proc. **234**, 95 (1991).
[36] P. S. de Baranda, A. K. Knudsen, and E. Ruh, J. Am. Ceram. Soc. **76**, 1761 (1993).
[37] V. D. Kagan and N. A. Red'ko, Proceedings of the 14th International Conference on Thermoelectrics in St. Petersburg, Russia, 1995, p. 78.
[38] P. G. Klemens, Proc. Phys. Soc., London, Sect. A **68**, 1113 (1955).